Development of a cyclin-dependent kinase inhibitor devoid of ABC transporter-dependent drug resistance

M Kaliszczak[1], H Patel[1], S H B Kroll[2], L Carroll[1], G Smith[1], S Delaney[1], D A Heathcote[1], A Bondke[2], M J Fuchter[2], R C Coombes[1], A G M Barrett[2], S Ali[1] and E O Aboagye*,[1]

[1]Faculty of Medicine, Department of Surgery and Cancer, Imperial College London, Hammersmith Hospital Campus, Du Cane Road, London W12 0NN, UK and [2]Department of Chemistry, Imperial College London, London SW7 2AZ, UK

Background: Cyclin-dependent kinases (CDKs) control cell cycle progression, RNA transcription and apoptosis, making them attractive targets for anticancer drug development. Unfortunately, CDK inhibitors developed to date have demonstrated variable efficacy.

Methods: We generated drug-resistant cells by continuous low-dose exposure to a model pyrazolo[1,5-a]pyrimidine CDK inhibitor and investigated potential structural alterations for optimal efficacy.

Results: We identified induction of the ATP-binding cassette (ABC) transporters, ABCB1 and ABCG2, in resistant cells. Assessment of features involved in the ABC transporter substrate specificity from a compound library revealed high polar surface area ($>100\,\text{Å}^2$) as a key determinant of transporter interaction. We developed ICEC-0782 that preferentially inhibited CDK2, CDK7 and CDK9 in the nanomolar range. The compound inhibited phosphorylation of CDK substrates and downregulated the short-lived proteins, Mcl-1 and cyclin D1. ICEC-0782 induced G2/M arrest and apoptosis. The permeability and cytotoxicity of ICEC-0782 were unaffected by ABC transporter expression. Following daily oral dosing, the compound inhibited growth of human colon HCT-116 and human breast MCF7 tumour xenografts *in vivo* by 84% and 94%, respectively.

Conclusion: We identified a promising pyrazolo[1,5-a]pyrimidine compound devoid of ABC transporter interaction, highly suitable for further preclinical and clinical evaluation for the treatment of cancer.

Cyclin-dependent kinases (CDK) are proteins that control progression through the cell cycle (Sherr, 1996). As core elements of the cell cycle machinery, cyclin D in complex with CDK4/6 and cyclin E in complex with CDK2 sequentially phosphorylate the retinoblastoma (Rb) protein facilitating transition from G1- to S-phase (Sherr, 1994). Moreover, fundamental to cell growth, cyclin A-CDK1/2 and cyclin B-CDK1 complexes allow progression through the S-phase and entry into mitosis (Pines, 1991). Phosphorylation of CDKs by the CDK-activating kinase complex comprises three subunits – CDK7, cyclin H and MAT1 – is a key step in the regulation of their activities (Harper and Elledge, 1998; Fisher, 2005; Lolli and Johnson, 2005). Deregulation of CDK expression or function via genetic or epigenetic mechanisms is a common feature of almost all types of cancer as well as other disease states (Malumbres and Barbacid, 2001). Besides its role in the regulation of the cell cycle, CDK7 is also required for transcription initiation by RNA polymerase II (polII). The CDK7/cyclinH/MAT1 complex and cyclin T–CDK9 promote initiation and elongation of nascent RNA transcripts by phosphorylating the carboxy-terminal domain of RNA polII (Prelich, 2002; Palancade and Bensaude, 2003; Meinhart *et al*, 2005). Because of their critical roles in the regulation of the cell cycle and transcriptional activity, as well as their impact on apoptotic pathways, CDKs comprise a favourable set of targets for anticancer drug development.

*Correspondence: Dr EO Aboagye; E-mail: eric.aboagye@imperial.ac.uk

The first generation of CDK inhibitors have entered late-stage clinical trials but so far have only shown modest activity due to unfavourable pharmacology. Although the mechanisms responsible for such poor pharmacology/potency in the clinic are not entirely clear, potential reasons may include drug efflux in the case of flavopiridol or poor metabolic stability in the case of R-roscovitine (seliciclib; CYC202) (Robey et al, 2001; Nutley et al, 2005). We have previously designed and optimised a number of pyrazolo[1,5-a]pyrimidine-based CDK inhibitors (Ali et al, 2009; Heathcote et al, 2010). Among these, BS-194 was found to be a very potent CDK inhibitor, with nanomolar activities against CDK1, 2, 7 and 9 (Heathcote et al, 2010; Figure 1A). This compound was efficacious in vitro against a panel of cancer cell lines from different origins and demonstrated antitumour activity in human xenograft models of colon and breast cancer (Heathcote et al, 2010). In the present study, in cells exposed long term to a CDK inhibitor, we reveal that drug-induced overexpression of the ATP-binding cassette (ABC) transporters – ABCB1 (also known as P-glycoprotein, P-gp) and ABCG2 (breast cancer-resistant protein) – constitutes a major mechanism of drug efflux in vitro and in vivo. This could be an important mechanism of resistance in future clinical trials. We identified unfavourable properties in the pyrazolo[1,5-a]pyrimidine series and, using that information, synthesised a novel orally active CDK inhibitor devoid of ABC transporter interaction that inhibits the growth of solid tumours in mice.

MATERIALS AND METHODS

Cells. HCT-116, A549 and MCF7 cells were obtained from the American Type Cell Culture Collection (Rockville, MD, USA) and authenticated by short tandem-repeat profiling under contract by DDC Medical (London, UK). A2780- and doxorubicin-resistant subclones A2780^{AD} were provided by the National Cancer Institute (Bethesda, MD, USA). 3T3 and 3T3 transfected with cDNA expressing P-gp (pHamdr1) were kindly provided by Dr E Schuetz from St Jude's Children Research Hospital (Memphis, TN, USA), and MCF7- and mitoxantrone (MX)-resistant subclones MCF7-MX by Dr E Schneider from the University of Maryland (Baltimore, MD, USA). All cells were passaged in our laboratory for fewer than 6 months on receipt.

Establishment of HCT-116 and MCF7 cell lines resistant to BS-194. Cells were originally grown in media containing BS-194 at 40 nM. When cells achieved 80% confluency, they were split and grown with raised stepwise concentration of BS-194 up to 200 nM in HCT-116 cells and up to 1.2 μM in MCF7 cells. HCT-116 cells acquired resistance within 2 weeks, whereas MCF7 cells developed substantial resistance after 3 months.

Cytotoxicity assay. Drug concentrations that inhibited 50% of cell growth (GI$_{50}$) were determined using a sulphorhodamine B technique as described elsewhere (Vichai and Kirtikara, 2006).

Determination of biophysical properties. The hydrophobicity of the molecules, LogP, the polar surface area (PSA, defined as the sum of surfaces of polar atoms, usually oxygens, nitrogens and their attached hydrogens) and the pKa were calculated using ACD labs version 12 software (Advance Chemistry Development Inc., Toronto, ON, Canada).

Determination of protein expression by flow cytometry. Collected HCT-116 cells were stained using the monoclonal antibody to ABCB1 (UlC2) and to ABCG2 (BXP-21) as previously described (Heathcote et al, 2010). Staining intensity was assessed by flow cytometry (FACS canto, Becton Dickinson, Mountain View, CA, USA) and analysed using the FlowJo software (Treestar Inc., Ashland, OR, USA). Results were expressed as a geometric mean.

Calcein-AM assay. Calcein-AM uptake and conversion to fluorescent calcein was determined using the Invitrogen calcein-AM assay kit according to the manufacturer's instructions (Invitrogen, Paisley, UK). Fluorescence was measured by flow cytometry using FACS canto and the intensity quantified by FlowJo software.

Immunoblotting. Cells were cultured for 24 h and subsequently treated with different compounds at the indicated concentrations for 24 h. Protein samples were subsequently prepared by lysing cells in RIPA buffer (Invitrogen) supplemented with protease and phosphatase inhibitor cocktails (Sigma, St Louis, MO, USA). Tumour samples were prepared as follows: excised and snap-frozen tumour xenografts were homogenised in RIPA lysis buffer with the PreCellys 24 homogeniser and CK14 bead-containing tubes (2 cycles of 25 s at 6500 r.p.m.; Bertin Technologies, Montigny-le-bretonneux, France) and subjected to standard western blot procedures.

Immunohistochemistry. Tumours treated with BS-194, ICEC-0782 or vehicle were excised after 14 days of treatment, fixed in formalin, embedded in paraffin and cut into 5.0-μm sections. Immunohistochemical staining was performed as described previously (Heathcote et al, 2010). Data from 10 randomly selected fields of view per section were captured using an Olympus BX51 microscope (Olympus UK Ltd, London, UK). Positive cells were counted using ImageJ software (NIH, Bethesda, MD, USA) and expressed as a percentage of total cells counted.

Immunofluorescence. Exponentially growing MCF7 and MCF7-MX cells were seeded in chamber slides on day 1. The cells were treated on day 2 with 1 μM of BS-194 or ICEC-0782 for 24 h and stained by immunofluorescence as described elsewhere (Kaliszczak et al, 2010).

Permeability assay. Permeability of test compounds was performed using the transwell assay as previously described (Kaliszczak et al, 2010).

Figure 1. Acquired resistance to BS-194 is associated with the expression of ABC transporters in HCT-116 and MCF7 cell lines. (**A**) Chemical structure of BS-194. (**B**) Growth inhibition of BS-194 in HCT-116 parental cells and in HCT-116 cells grown in the presence of BS-194 (HCT-116-BS-194R) as determined by the sulphorhodamine B assay. (**C**) Levels of ABCB1 expression as determined by flow cytometry in HCT-116 and HCT-116-BS-194R cells. Results are expressed as geometric mean of the fluorescence intensity. (**D**) Functional expression of ABCB1 in HCT-116 and HCT-116-BS-194-R cells as determined by differential uptake of fluorescent dye calcein and flow cytometry. (**E**) Levels of ABCG2 expression as determined by flow cytometry in HCT-116 and HCT-116-BS-194R cells compared with expression in ABCG2-positive MX-resistant cells (MCF7-MX). (**F**) Growth inhibitory effect of BS-194 in MCF7 parental cells and in MCF7 cells grown in the presence of BS-194 (MCF7-BS-194R). (**G**) ABCG2 and ABCB1 expression in MCF7-BS-194R cells as determined by western blotting. Cells were grown in stepwise increasing concentration of the drug over several passages (p2 to p15). Phamdr1 cells are positive for ABCB1 and negative for ABCG2. (**H**) ABCB1 expression in HCT-116 xenografts excised after 14 days of treatment with BS-194 at 25 mg kg^{-1} per day (p.o.) as determined by immunohistochemistry. Results are expressed as a percentage of positive cells (n = 3 tumours per group). (**I**) ABCG2 expression in MCF7 xenografts excised after 14 days of treatment with BS-194 at 20 mg kg^{-1} per day (i.p.) as determined by immunohistochemistry. Results are expressed as a percentage of positive cells (n = 3 tumours per group). Scale bar, 50 μm (*P < 0.05, ***P < 0.0001).

***In vitro* kinase assays.** Purified recombinant CDK1/cycB1, CDK2/cycE, CDK4/cycD1, CDK5/p35NCK, CDK6/CycD1, CDK7/CycH/MAT1 and CDK9/CycT were purchased from Proqinase GmbH

(Freiburg, Germany). Kinase assays were performed as described previously (Ali *et al*, 2009), using substrate peptides purchased from Proqinase GmbH. Measurement of the amount of ATP
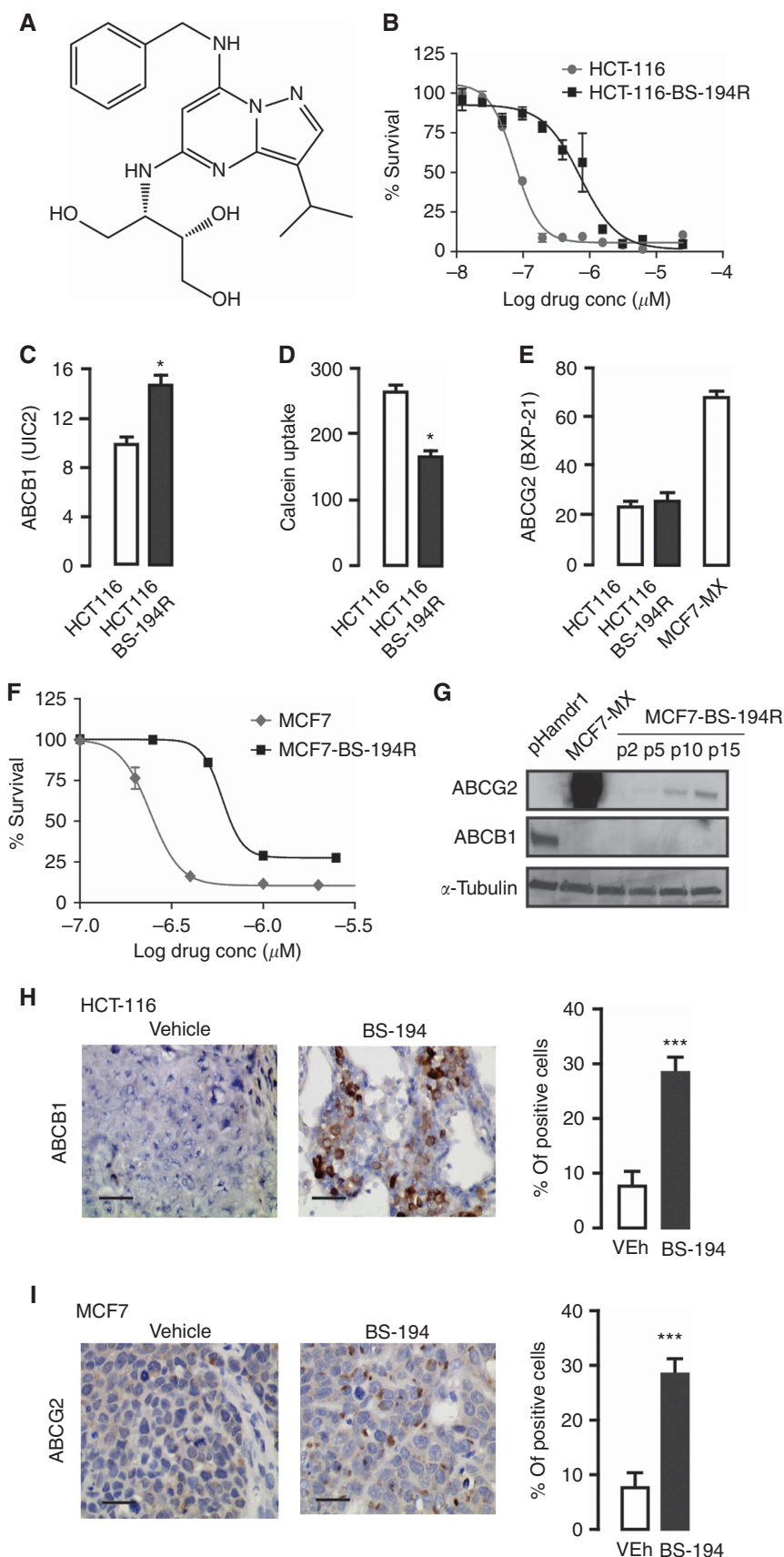
remaining at the end of the reaction, carried out with a luciferase assay (PKLight assay; Cambrex, Nottingham, UK), was used to determine inhibition of kinase activity by compounds.

Microsomal stability. Compounds ($5 \mu M$, final concentration) were incubated with a mixture 0.1 M Tris buffer (Sigma; prepared with double-distilled water, pH 7.4), 1 mM NADPH (Sigma) and $1 \, mg \, ml^{-1}$ human or mouse pooled liver microsomes or S9 fractions (BD Biosciences, Oxford, UK) for 1 h at 37 °C in a total volume of $250 \mu l$. For each sample, proteins were precipitated with ice-cold methanol ($3 \times$ volume), centrifuged, resuspended in mobile phase and filtered ($0.2 \mu m$) before HPLC–UV analysis.

Cell cycle analysis. Cells were treated with ICEC-0782 for 24 h. Collected cells were fixed with ethanol and stained with propidium iodide (Sigma) in PBS for 3 h. Cell cycle distributions were determined using flow cytometry (FACS canto, Becton Dickinson) and analysed using the FlowJo software.

Caspase 3/7 assay. Caspase 3/7 activity was determined using Promega's caspase 3/7 assay according to the manufacturer's instructions (Promega, Madison, WI, USA). Briefly, cells were transferred to white opaque 96-well plates, incubated for 1 h with Caspase-Glo reagent and the enzymatic activity of caspase 3/7 was measured using a TopCount NXT microplate luminescence counter (PerkinElmer, Shelton, CT, USA) and normalised to protein content.

Tumour xenografts. HCT-116 cells (5×10^6) were injected subcutaneously in $100 \mu l$ volume into the flank of female nu/nu-BALB/c athymic nude mice. Tumour measurements were performed daily and volumes were calculated using the formula (length (mm)) $\times$ (width (mm)) $\times$ (depth (mm)) $\times \pi/6$. Treatment with different compounds was initiated when tumours reached a volume of 50–100 mm^3. Throughout the 14-day treatment period, animal weights and tumour volumes were determined daily. All animal experiments were done by licensed investigators in accordance with the United Kingdom Home Office Guidance on the Operation of the Animal (Scientific Procedures) Act 1986 (HMSO, London, United Kingdom, 1990) and within guidelines set out by the United Kingdom National Cancer Research Institute Committee on Welfare of Animals in Cancer Research (Workman et al, 2010).

[18F]Fluorothymidine positron emission tomography imaging. Approximately 100 mm^3 HCT-116 tumour-bearing mice were treated with ICEC-0782 at $15 \, mg \, kg^{-1}$ BID or with vehicle. At 48 h post treatment, the animals were scanned on a dedicated small animal positron emission tomography (PET) scanner (Siemens Inveon PET module; Siemens, Erlangen, Germany) following a bolus intravenous injection of ~ 3.7 MBq of [18F]Fluorothymidine ([18F]FLT) as previously described (Leyton et al, 2006; Pisaneschi et al, 2010; Kaliszczak et al, 2013). The uptake value normalised to the injected dose at 60 min (%ID ml^{-1} at 60 min) post injection extracted from time activity curves was used for comparisons (Pisaneschi et al, 2010).

Ki-67 immunostaining. Tumours treated with ICEC-0782 or vehicle were excised after imaging, fixed in formalin, embedded in paraffin and cut into 5.0-μm sections, and tumour proliferation was determined as previously described (Leyton et al, 2006). Data from 10 randomly selected fields of view per section were captured using an Olympus BX51 microscope at $\times 400$ magnification. Ki-67-positive cells were counted using the ImageJ software and expressed as a percentage of total cells counted.

Statistical analyses. Two tailed Student's t-tests were performed using GraphPad prism software (GraphPad, La Jolla, CA, USA), and P values< 0.05 using a 95% confidence interval were considered significant. Data are reported as mean $\pm$ s.e.m. of at

least three independent experiments unless otherwise stated. *$P < 0.05$, **$P < 0.005$ and ***$P < 0.0001$ were considered to be statistically significant; NS, not significant.

Additional methods. Synthesis and characterisation of compounds, HPLC–UV method and pharmacokinetic profiling are described in Supplementary Materials and Methods.

RESULTS

Tumours treated with continuous low-dose BS-194 develop resistance mediated by ABC transporters ABCB1 and ABCG2. To elucidate potential mechanisms of resistance to pyrazolo [1,5-a]pyrimidine CDK inhibitors, HCT-116 cells were grown in vitro and incubated with an increasing concentration of a representative CDK inhibitor, BS-194. After 2 weeks of continuous treatment, HCT-116 cells became 10-fold more resistant to BS-194 (Figure 1B). We evaluated the levels of the major ABC transporters involved in the multi-drug resistance (MDR) phenotype and found that ABCB1 was upregulated by 1.7-fold in HCT-116 cells resistant to BS-194 (HCT-116-BS-194R; Figure 1C). The functional activity of the transporter was further characterised using the ABCB1 substrate calcein-AM that is converted to its fluorescent dye calcein within the cell; HCT-116-BS-194R cells were associated with 1.5-fold less intracellular calcein than their parental counterparts (Figure 1D). Levels of ABCG2 were not altered (Figure 1E). Similarly, we generated MCF7 cells resistant to BS-194 (MCF7-BS-194R) that were 2.5-fold more resistant to BS-194 than the parental MCF7 cells when comparing their GI$_{50}$ (Figure 1F). Lower potency was also observed at the highest concentration tested (i.e., 2.5 μM); 28% of the MCF7-BS-194R cells survived compared with 10% of the parental cells. Progressive transformation of MCF7-BS-194R cells over 3 months was associated with an increase of ABCG2 protein levels, which is relatively low compared with MX-resistant cells (MCF7-MX) that were generated over 9 months (Nakagawa et al, 1992; Ross et al, 1999; Figure 1G). No differences in ABCB1 protein levels were observed.

To verify whether our initial findings had relevance in vivo, we evaluated the protein expression of ABCB1 in HCT-116 and ABCG2 in MCF7 tumour-bearing mice treated with BS-194 over 14 days. Both transporters were upregulated by threefold in the treated group (Figure 1H and I).

BS-194 is a substrate of the ABC transporters ABCG2 and ABCB1. We next investigated whether BS-194 is a substrate of the ABC transporters and actively effluxed from cells. In MCF7 cells, treatment with BS-194 at 1 μM for 24 h abolished the phosphorylation of polII at ser5, a marker of CDK7 inhibition (Figure 2A). In MCF7-MX cells that overexpressed ABCG2, similar treatment with BS-194 did not reduce polII phosphorylation. When treated continuously for 72 h, MCF7-MX cells were 15 times more resistant to their parental counterparts with respect to growth (Figure 2B). Similarly, pHamdr1 cells, which are 3T3 cells stably transfected with a mdr1 cDNA (overexpressing ABCB1), were 10-fold more resistant to BS-194 than their paired isogenic 3T3 counterparts (Figure 2C). Cross-resistance to BS-194 mediated by ABCB1 was also demonstrated in A2780^{AD} ovarian cancer cells that are resistant to doxorubicin (Supplementary Figure S1).

To evaluate whether ABCG2 and ABCB1 could impair cellular absorption of BS-194, we used human caco-2 monolayers and determined the ratio between secretion and absorption. The ratio for BS-194 was 12 (Figure 2D), demonstrating active efflux (ratio > 3) (Szakacs et al, 2006). Pretreatment with an ABCG2 inhibitor, FTC, and the ABCB1 inhibitor, verapamil, reduced the ratio to 2.5. As a positive control, vinblastine, an ABCB1 substrate, showed a permeability ratio of 8 that was reduced to 3 following pretreatment with verapamil.
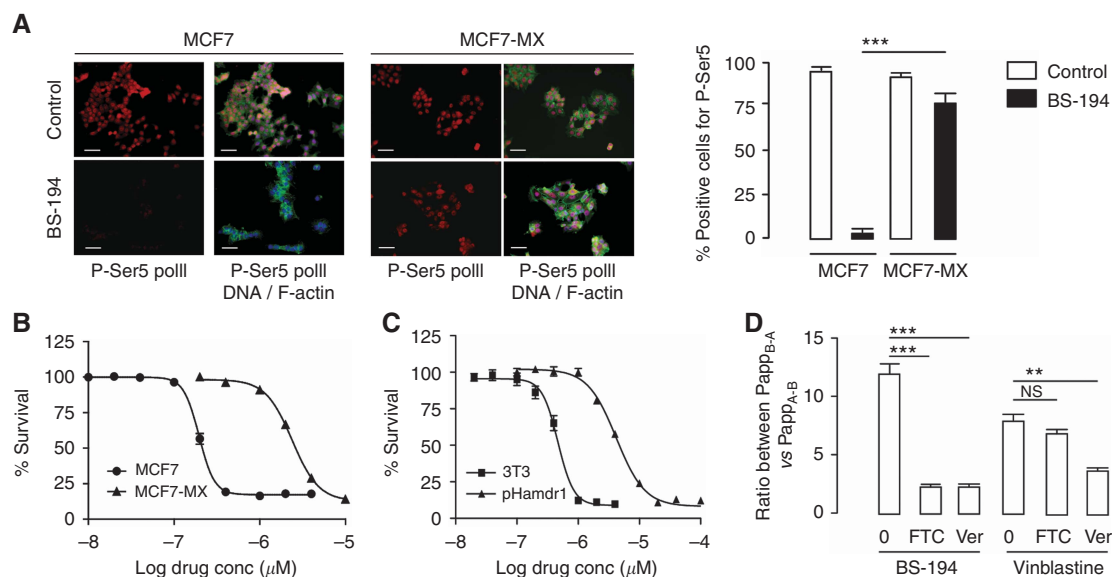
Figure 2. BS-194 is a substrate of the ABC transporters ABCG2 and ABCB1. (**A**) MCF7 and MCF7-MX cells (overexpressing ABCG2) were treated with BS-194 at 1 μM for 24 h and stained for phospho-ser5 of polII (red). DAPI staining (DNA) is represented in blue and phalloidin (F-actin) in green. Scale bar, 20 μm. Staining intensities were expressed as percent positive cells per field using 10 random fields of view per chamber slide ($n = 3$, *** $P < 0.0001$). (**B**) Growth inhibitory effect of BS-194 in MCF7 cells and MCF7-MX cells. (**C**) Growth inhibitory effect of BS-194 in phamdr1 cells overexpressing ABCB1 (3T3 mice fibroblasts transfected with a vector containing human *mdr1*) and in 3T3 cells (transfected with an empty vector). (**D**) Permeability ratios of BS-194 as determined by transwell assay. Results are expressed as ratios of secretion (from the basal to the apical side; $Papp_{B–A}$) to absorption (from the apical to the basal side; $Papp_{A–B}$). Cells were incubated with BS-194 at 10 μM with or without addition of inhibitors for ABC transporters (FTC for ABCG2 and verapamil for ABCB1, both at 10 μM). Permeability ratios of vinblastine (at 10 μM), a substrate for ABCB1 but not for ABCG2, are also represented (mean ± s.e.m.; $n = 3$ independent repeats; **$P = 0.0012$, ***$P < 0.0001$, NS, not significant).

High PSA is a major determinant of the interaction of pyrazolo[1,5-*a*]pyrimidine derivatives with ABCG2 and ABCB1. We examined other members of our pyrazolo[1,5-*a*]pyrimidine inhibitor family to assess trends that impact on ABC transporter-mediated efflux. We previously developed another CDK inhibitor, BS-181, with preferential low nanomolar affinity for CDK7 (Ali *et al*, 2009). This compound was, however, associated with an unfavourable pharmacokinetic profile that precluded oral administration. BS-181 was equipotent in A2780^{AD} cells, overexpressing ABCB1, and in their parental counterpart, suggesting that the compound was not a substrate of the transporter (Supplementary Figure S1). We screened our library of pyrazolo[1,5-*a*]pyrimidine CDK inhibitors to identify non-substrates of the ABC transporters with potentially favourable absorption and clearance properties, and satisfactory metabolic stability, to assure adequate systemic exposure to elicit a pharmacodynamic response (Ali *et al*, 2009). Fifteen compounds with nanomolar CDK activity were selected for further investigation (Supplementary Figure S2 and Supplementary Table S1).

To test ABCG2 substrate specificity, we evaluated the differential growth inhibitory effect of the series in MCF7-MX cells (overexpressing ABCG2) and their parental counterparts. We found that in addition to BS-194, its diastereoisomer, BS-195 and ICEC-0187 (Supplementary Figure S2), were associated with GI$_{50}$ ratios >2 (Figure 3A). From previous structure activity relationship (SAR) studies, substrates of ABC transporters share a common set of properties such as a high molecular weight (MW >500), >2 aromatic rings, >8 nitrogen and oxygen (N + O) atoms, a lipophilicity (Log*P*) between 1 and 5, a pKa >4 and a PSA >85 Å^2 (Didziapetris *et al*, 2003; Varma *et al*, 2005; Kaliszczak *et al*, 2010). Amongst our pyrazolo[1,5-*a*]pyrimidine series, we identified a high PSA as a common property shared by BS-194, BS-194 and ICEC-0187 (Supplementary Table S2). We hypothesised that the cut-off value should range between

84 Å^2 (associated with ICEC-0067, a non-substrate) and 104 Å^2 (associated with ICEC-0187, a substrate).

Similarly, to test ABCB1 substrate specificity we evaluated the differential growth inhibitory effect in pHamdr1 cells (overexpressing ABCB1) and their isogenic counterparts, and found that in addition to BS-194, BS-195 and ICEC-0187 were associated with ratios >2 (Figure 3B). The impact of another major ABC transporter, MRP1, on the growth inhibitory effect of the pyrazolo[1,5-*a*]pyrimidine derivatives was also evaluated in A549 cells (Pham *et al*, 2009). No difference in growth inhibition was seen when the cells were treated with a specific inhibitor of MRP1, MK-571 (Supplementary Figure S3), indicating that these compounds are not a substrate for MRP1.

Pyrazolo[1,5-*a*]pyrimidine derivatives with a pKa <7.4 are associated with favourable permeability. Although BS-181 is not a substrate for the ABC transporters, it is poorly absorbed; its chemical structure contains a primary amine that would be charged at physiological pH, this feature would be predicted to reduce membrane permeability. To test whether this could be a feature common to highly basic pyrazolo[1,5-*a*]pyrimidine derivatives, we evaluated their permeability across the caco-2 cells ($Papp_{A–B}$). All the compounds with a calculated pKa >7.4 (charged at physiological pH) were poorly absorbed ($Papp_{A–B}$ $< 3 \times 10^{-6}$ cm s^{-1}) (Figure 3C). ICEC-0186 has a calculated pKa <7.4 but was associated with a poor permeability, indicating either that pKa alone does not explain permeability or perhaps due to conversion of ICEC-0186 to a charged entity in the course of the experiment. Of the remaining compounds with a calculated pKa <7.4, ICEC-0063 and ICEC-0067 were associated with high permeability ($Papp_{A–B}$ $> 10 \times 10^{-6}$ cm s^{-1}). In contrast, BS-195 and BS-194, with pKa <7.4, were actively effluxed by the ABC transporters (Figure 3A and B), in turn limiting their absorption (Figure 3C and D).
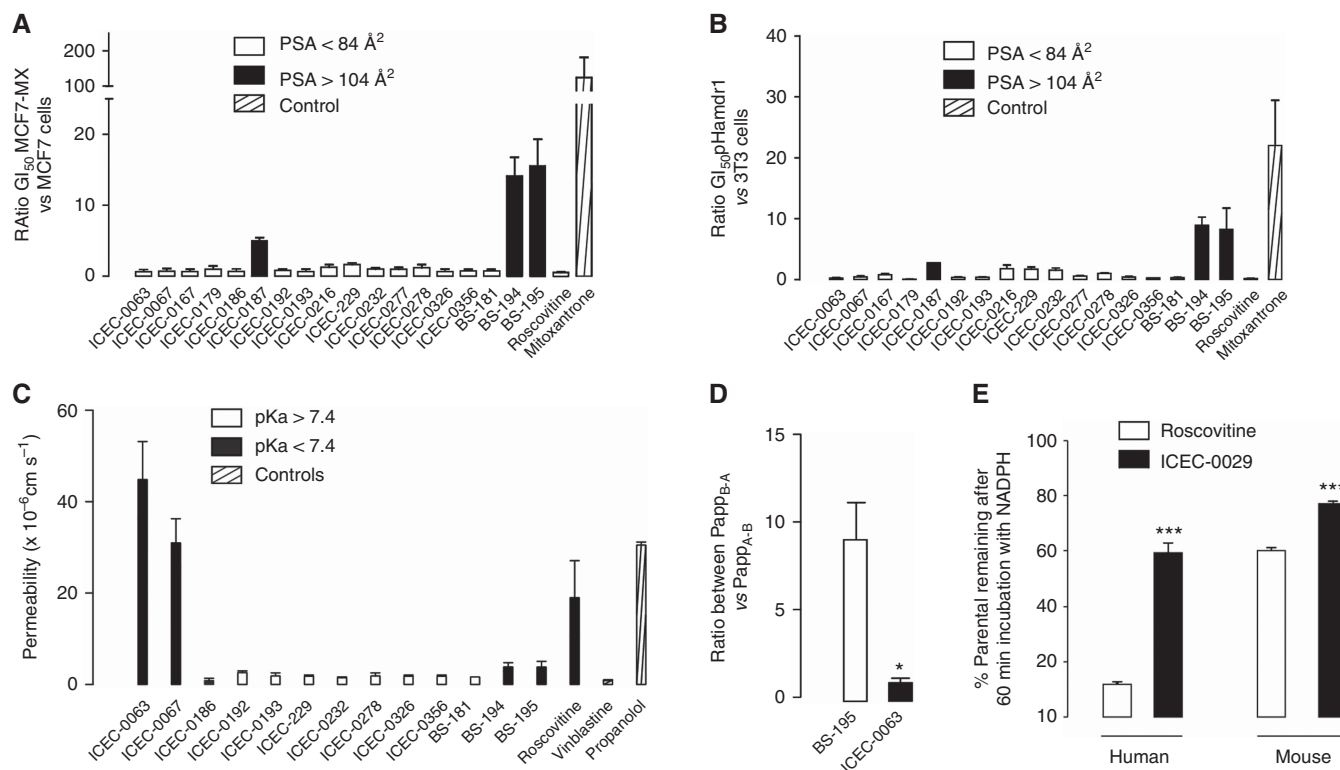
Figure 3. Physicochemical determinants of ABC transporter substrate specificity, metabolism and permeability in the pyrazolo[1,5-a]pyrimidine series of CDK inhibitors. (**A** and **B**) Compound selectivity expressed as the ratios of GI_{50} (growth inhibition at 50%) in ABCG2- (**A**) and ABCB1- (**B**) overexpressing cells to that in parental cells. Results are mean ± s.e.m. of three experiments each performed in six replicates. Compounds were colour coded according to their PSA. (**C**) Permeability of the compounds tested at $10\,\mu M$ as determined by the transwell assay. Compounds were classified according to their pKa. A value of 7.4 was chosen as a cut-off value. Vinblastine and propanolol were assessed for comparison. (**D**) Permeability ratios ($Papp_{B-A}$ over $Papp_{A-B}$) of BS-195 compared with ICEC-0063 ($n = 3$ independent repeats, $*P = 0.015$). (**E**) Metabolic stability of roscovitine compared with ICEC-0229 in human and mouse microsomes ($n = 3$ independent repeats, $***P < 0.0001$).

Metabolic stability of the pyrazolo[1,5-a]pyrimidine series. Roscovitine, a CDK inhibitor in clinical trials, undergoes rapid metabolism in mice and in human, primarily via an NADPH cytochrome P450 oxidoreductase-dependent process (de la Motte and Gianella-Borradori, 2004; Nutley et al, 2005). Some of those metabolites have been synthesised and shown to be much less potent than the parent compound at inhibiting CDK2 (Nutley et al, 2005). Among the pyrazolo[1,5-a]pyrimidine derivatives, we identified three classes of compounds: highly metabolised compounds with <10% of parent compound remaining after 60 min incubation of drug with NADPH and mouse S9 fractions (ICEC-0067, ICEC-0063, ICEC-0179 and ICEC-0186; roscovitine); compounds with intermediate stability showing >10% but <50% of parent compound (ICEC-0167 and ICEC-0187); and stable compounds with >50% of parent compound remaining, including ICEC-0229 (Supplementary Table S3). Similar classification of the series could have been made with mouse microsomes and human microsomes/S9 fractions, but with different thresholds.

Lead identification, optimisation and characterisation. Among the pyrazolo[1,5-a]pyrimidine derivatives, ICEC-0229 was identified as a lead. It was associated with a mean GI_{50} of $1\,\mu M$ when tested in HCT-116, MCF7 and A549 cancer cells (Supplementary Table S4). It was also found not to be a substrate of the ABC transporters and its metabolic stability was sixfold greater than that for roscovitine (Figure 3E). However, it possessed unfavourable permeability properties due to its charge (pKa = 10.5) that prompted the development of analogues of ICEC-0229 that would be uncharged at physiological pH. Six carbamate derivatives were synthesised and tested for their growth inhibitory potency in A549

cells (Figure 4A). We found that the length of the aliphatic side chain was inversely proportional to the biological activity, thus identifying ICEC-0782 as the most potent carbamate. Using recombinant enzymes, when compared with ICEC-0229, ICEC-0782 lost preferential selectivity against CDK7 (16-fold), but gained 3.6-fold higher CDK2 potency and, to a lower extent, CDK9 (1.7-fold) potency (Figure 4B). Of note, CDK7, CDK2 and CDK9 enzyme inhibition potency remained within the nanomolar range (170, 71 and 440 nM, respectively). In HCT-116 cells, treatment with ICEC-0229 or ICEC-0782 for 24 h dose dependently inhibited phosphorylation of polII at ser2, a marker of CDK9 inhibition (Figure 4C). Short-lived anti-apoptotic protein Mcl-1 and cell cycle-regulated protein cyclin D1 were probably inhibited as a consequence of polII inhibition (Shapiro, 2006).

To test whether the carbamate derivative had an improved permeability over its parent compound containing a primary amine, the absorption of ICEC-0782 was tested across caco-2 cells using the transwell assay. ICEC-0782 was associated with a 10-fold greater permeability than ICEC-0229 (Figure 4D). ICEC-0782, with a PSA of $95\,\text{Å}^2$, was associated with a permeability ratio close to 1, suggesting a lack of active efflux (Figure 4E). This permitted further refinement of the cut-off value of PSA for the prediction of ABC transporters' substrate specificity of the pyrazolo[1,5-a]pyrimidines to $100\,\text{Å}^2$. ICEC-0782 was found to be potent at inhibiting polII phosphorylation at ser5 (at $1\,\mu M$ for 24 h), a marker of CDK7 inhibition, in MCF7-MX cells (overexpressing ABCG2; Figure 4F), unlike BS-194 (Figure 2A). When treated at $1\,\mu M$ for 72 h, MCF7-MX cells were 1.5-fold more sensitive to ICEC-0782 than for BS-194 (Figure 4G). The better potency of ICEC-0782 over BS-194 was also demonstrated in HCT-116-BS-194R (i.e., 1.3-fold when tested at both $0.5\,\mu M$ and $1\,\mu M$; Figure 4H).
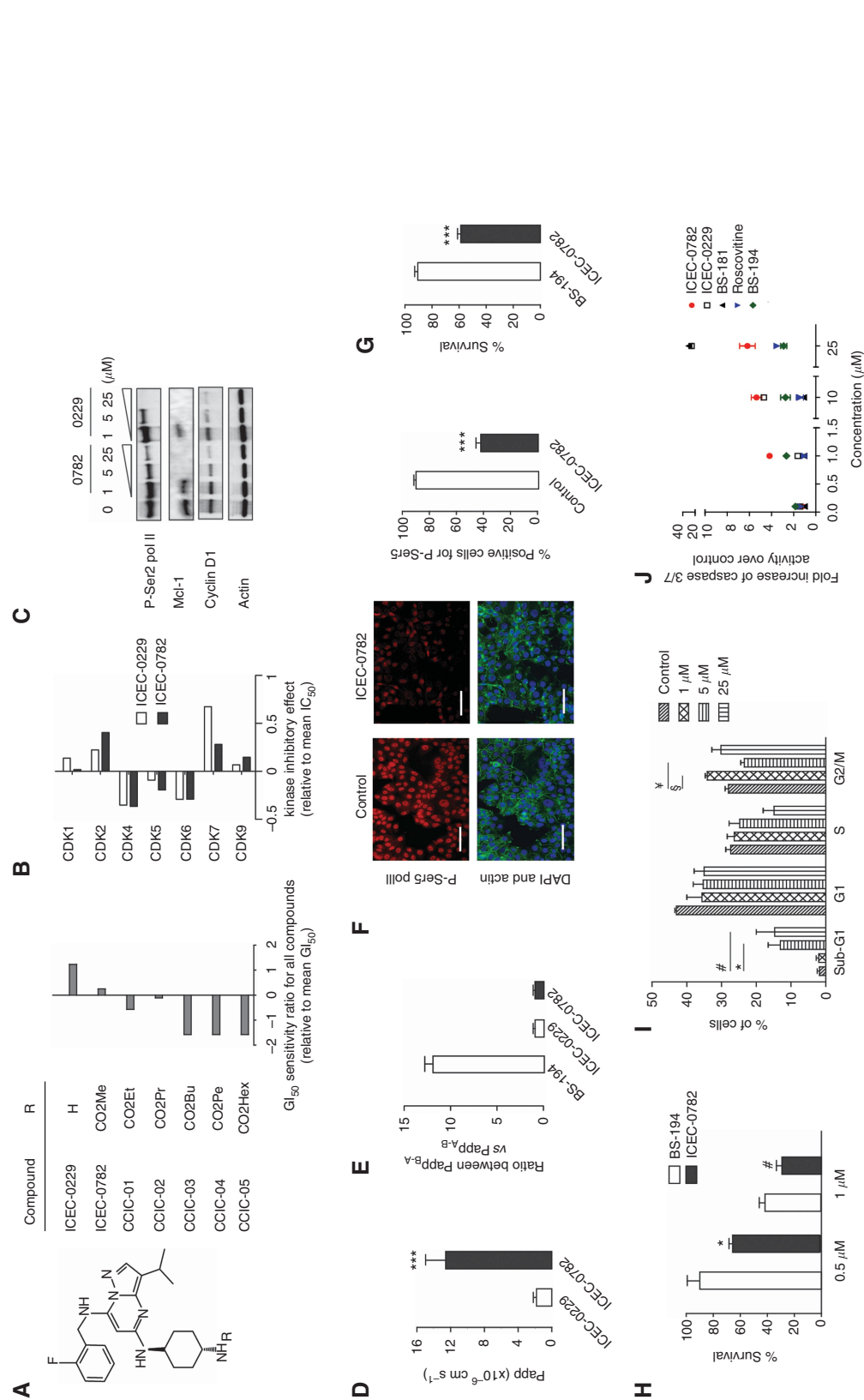
Figure 4. Lead optimisation of ICEC-0229 and characterisation of ICEC-0782. (**A**) Relative sensitivity of A549 cells to carbamate derivatives of ICEC-0782. (**A**) Relative sensitivity of A549 cells to carbamate derivatives of ICEC-0229. Values are expressed relative to the mean across all tested compounds. Mean GI$_{50}$ value for compounds (vertical line) tested was 40×10^{-6} M. (**B**) Relative kinase inhibitory effect of ICEC-0229 compared with its carbamate derivative ICEC-0782. Values are expressed relative to the mean across all inhibitors tested. Mean IC$_{50}$ value for compounds (vertical line) tested was 1×10^{-6} M. (**C**) Drug concentration-dependent effect of ICEC-0782 or ICEC-0229 on phosphorylation of polI at ser2 and expression Mcl-1 and cyclin D1 in HCT-116 cells after 24 h treatment. (**D**) Permeability of ICEC-0229 compared with ICEC-0782 as determined by the transwell assay ($n = 3$ independent repeats, ***$P < 0.0001$). (**E**) Active transport of BS-194, ICEC-0229 and ICEC-0782 mediated by ABC transporters across caco-2 cells, expressed as permeability ratios ($n = 3$ independent repeats, ***$P < 0.0001$). (**F**) Representative immunofluorescence illustrating the effect of ICEC-0782 (at 1 μM for 24 h) on phosphorylation of polII at ser5 (red) in MCF7-MX cells. Blue and green fluorescence represent DAPI staining (DNA) and phalloidin (F-actin), respectively. Scale bar, 100 μm. Staining intensities were expressed as per cent positive cells per field using 10 random fields of view per slide ($n = 3$ independent repeats, ***$P < 0.0001$). (**G**) Growth inhibitory effect of ICEC-0782 and BS-194 (both at 1 μM for 72 h) in MCF7-MX cells (***$P < 0.0001$). (**H**) Growth inhibitory effect of ICEC-0782 and BS-194 (at the indicated concentration for 72 h) in HCT-116-BS-194-R cells ($n = 3$ independent repeats, *$P = 0.031$, #$P = 0.037$). (**I**) Drug concentration-dependent effect of ICEC-0782 on cell cycle distribution in HCT-116 cells treated for 24 h ($n = 3$ independent repeats, *$P = 0.026$, #$P = 0.013$, $^{\S}P = 0.019$, $^{¥}P = 0.031$). (**J**) Drug concentration-dependent effect of inhibitors (incubated for 24 h) on caspase 3/7 activity in HCT-116 cells.

The growth inhibitory effect of ICEC-0782 was tested in native HCT-116 cells and found to be of similar potency as in MCF7 cells with GI_{50} of 3.2 and 4.2 μM, respectively (Supplementary Table S4). The cellular effect of ICEC-0782 was further characterised in HCT-116 cells to investigate the mechanism of growth inhibition. Flow cytometry studies showed that treatment of cells with ICEC-0782 for 24 h increased the G2/M population at the lowest concentration tested, i.e., 1 μM (from 28% in untreated cells to 34%), probably due to blockage of CDK7-induced activation of CDK1 (Shapiro, 2006). Cells also accumulated a sub-G1 fraction in a drug-concentration-related manner (from 1.5% in untreated cells to 15% at the highest concentration tested, i.e., 25 μM; Figure 4I), suggesting an apoptotic mechanism. We confirmed the drug-induced increase in sub-G1 as occurring via apoptosis by measuring the caspase 3/7 activity: ICEC-0782 induced a drug-concentration-related increase in caspase 3/7 activity (Figure 4J). BS-181 also induced caspase 3/7 activation, but only at the highest concentration tested (i.e., 25 μM).

Pharmacokinetic profile of ICEC-0782 favours *in vivo* antitumour activity. We examined the pharmacokinetic advantage of ICEC-0782 over ICEC-0229. When given orally at 10 mg kg^{-1}, maximum drug concentration (C_{max}) of ICEC-0782 was achieved rapidly (15 min) in contrast to that with ICEC-0229 (120 min; Figure 5A and B). The C_{max} and the drug exposure (AUC_{0-24h}) were, respectively, 13- and 6.5-fold greater than for ICEC-0229. The bioavailability of ICEC-0782 was also improved by 2.2-fold (from 19% to 42%). The drug was relatively stable *in vivo* with a plasma half life of 165 min.

Next, we tested whether the potent *in vitro* activity of ICEC-0782 combined with its favourable pharmacokinetic features, favoured efficacy in the human cancer xenograft models. ICEC-0782 was tested in human colon cancer (HCT-116) xenograft model. Significant efficacy was obtained when given orally (p.o.) at 15 mg kg^{-1} BID (i.e., 30 mg kg^{-1} per day; Figure 5C). At this dose, ICEC-0782 treatment was associated with a tumour growth delay (TGD_{2x}) of 6.6 ± 1.2 days and a tumour growth inhibition (TGI) of 84% compared with vehicle; there was no general toxicity as

determined by changes in body weight (Supplementary Figure S4). ICEC-0782 was also tested in human breast cancer (MCF7) xenograft model. The drug was associated with a TGI of 92% compared with vehicle when given p.o. at 15 mg kg^{-1} BID (Figure 5D); TGD_{2x} could not be calculated.

***In vivo* antitumour activity of ICEC-0782 is associated with molecular and imaging biomarker changes.** Biochemical target modulation *in vivo* was determined by measuring levels of the phosphorylated form of Rb protein as a surrogate marker for CDK2 inhibition and phosphorylated forms of polII (at ser2 – a marker for CDK9 inhibition; and at ser5 – for CDK7). Levels of P-Rb, P-ser2 and P-ser5 were lower in HCT-116 tumours following 14 days treatment with ICEC-0782 at 30 mg kg^{-1} per day compared with vehicle (Figure 6A). Target modulation (e.g., decrease in the levels of P-Rb) was also seen in the MCF7 xenograft model (Supplementary Figure S5).

In PET studies, radioactivity in tumour regions normalised to the injected dose was used quantitatively to compare the effects of ICEC-0782 (Pisaneschi *et al*, 2010). There was a 1.4-fold decrease in tumour [^{18}F]FLT uptake in animals treated with ICEC-0782 for 48 h compared with vehicle-treated mice. The tumour uptake was 13.9 ± 0.9 before treatment and decreased to 10 ± 0.8 %ID ml^{-1} ($P = 0.005$) at 48 h after initiating treatment (Figure 6B). Ki-67 immunostaining decreased in these tumours in keeping with the reduction in tumour [^{18}F]FLT uptake (1.3-fold; $P = 0.014$; Figure 6C).

It is noteworthy that the MDR phenotype characterised by the expression of ABC transporters was neither induced in HCT-116 tumours (Figure 6D) nor in MCF7 tumours (Supplementary Figure S6) after 14 days ICEC-0782.

DISCUSSION

We have developed a novel, orally active pyrazolo[1,5-*a*]pyrimidine nanomolar CDK inhibitor, ICEC-0782, that inhibits tumour
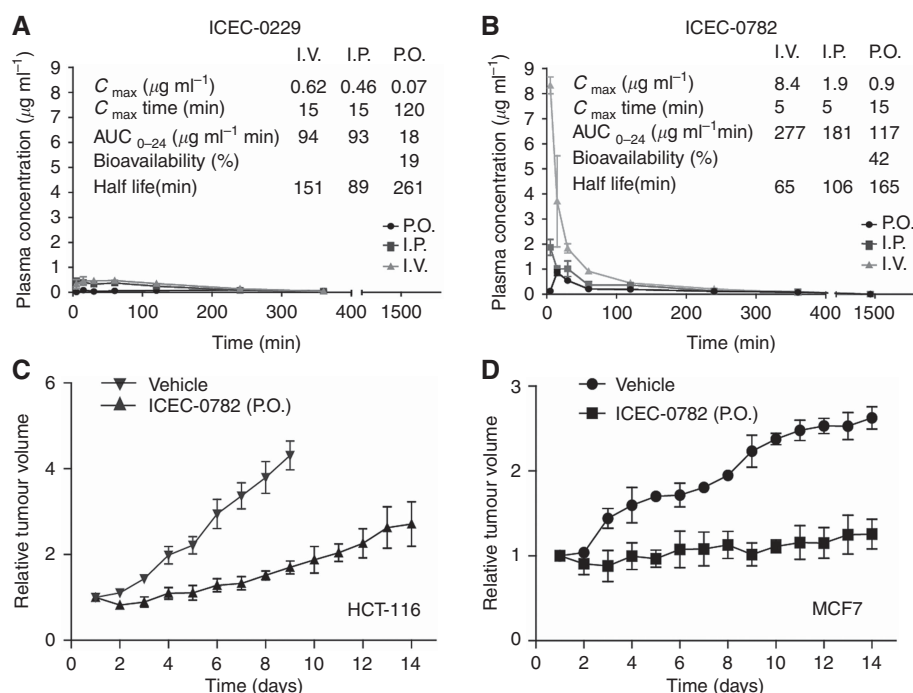
Figure 5. ICEC-0782 has improved pharmacokinetic profile over ICEC-0229 and demonstrates antitumour activity. (**A** and **B**) Pharmacokinetic profiles of ICEC-0229 (**A**) and ICEC-0782 (**B**) after a single injection at 10 mg kg^{-1} ($n = 3$ mice). Three routes of injection (i.p., i.v. and p.o.) are shown. (**C** and **D**) Effect of ICEC-0782 on tumour growth in human colon HCT-116 (**C**) and in human breast MCF7 xenograft (**D**) models ($n \geqslant 5$ tumours). ICEC-0782 was dosed orally twice daily (BID) at 15 mg kg^{-1} every day for 14 days.
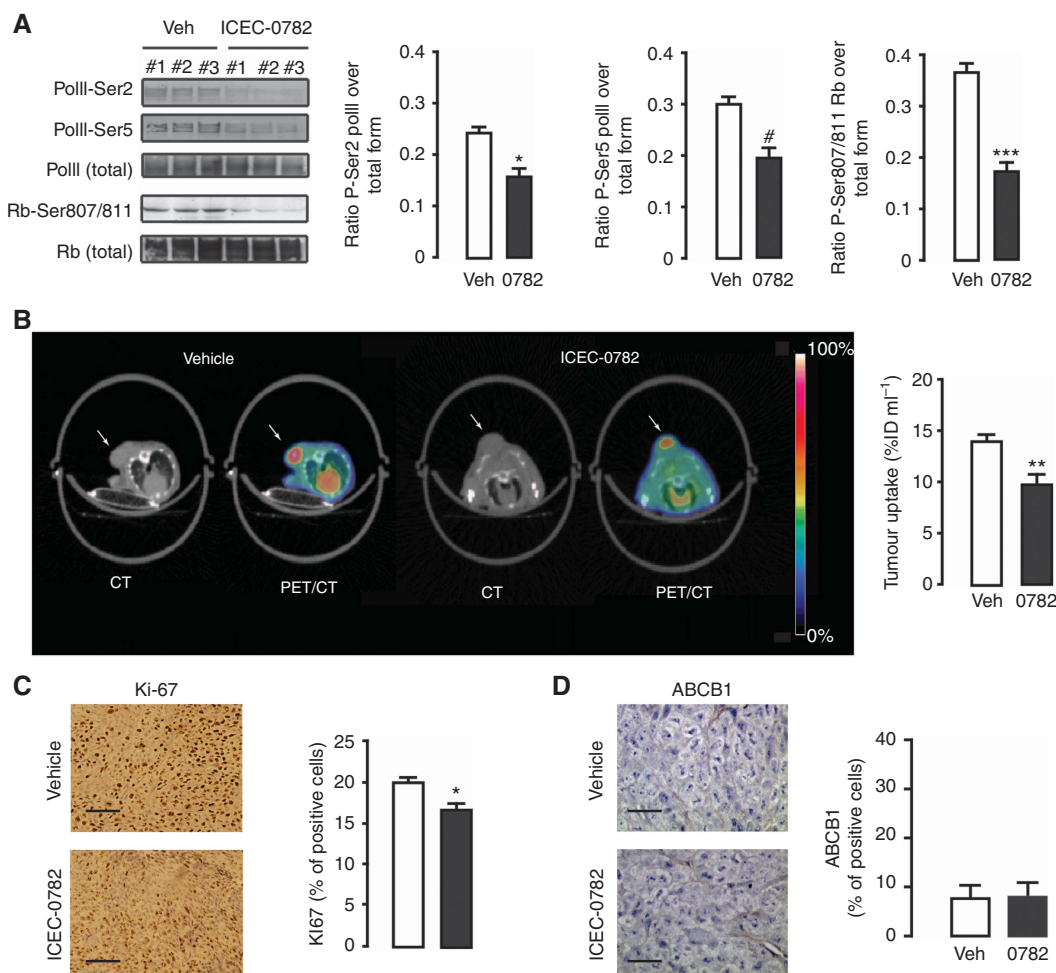
Figure 6. Molecular and imaging biomarkers for monitoring pharmacodynamics of ICEC-0782 in HCT-116 xenografts. (**A**) Effect of ICEC-0782 on the phosphorylated form of Rb (at ser807/811) and polII (at ser2 and ser5). HCT-116 tumours were excised after 14 days of oral treatment at 15 mg kg^{-1} BID. Quantification of the phosphorylated proteins relative to total protein by densitometry ($n = 3$ tumours, *$P = 0.037$, #$P = 0.041$, ***$P < 0.0001$). (**B**) Effect of ICEC-0782 on [^{18}F]FLT after 2 days of oral treatment at 15 mg kg^{-1} BID. Computed tomography (CT; left) and corresponding [^{18}F]FLT–PET–CT (right). For visualisation, cumulative images up to 60 min are displayed. The tumour is indicated by an arrow. Quantitative [^{18}F]FLT uptake at 48 h was expressed as radiotracer uptake in tumours normalised to the injected dose and expressed as %ID ml^{-1} of tissue ($n = 4$ tumours, **$P = 0.005$). (**C**) Ki-67 immunostained tumour sections after treatment for 2 days. Proliferative cells have brown staining. Ki-67 labelling index was calculated from 10 random fields of view per slice (two slices per tumour and three tumours per group). *$P = 0.014$. The Ki-67-positive cells were expressed as a percentage of total cells. Scale bar, 100 μm. (**D**) ABCB1 expression in tumours excised after 14 days of treatment with ICEC-0782. Results are expressed as a percentage of positive cells ($n = 3$ tumours per group). Scale bar, 50 μm.

growth and is devoid of the induction of MDR phenotype. Cyclin-dependent kinases are promising targets in cancer therapeutics because of their key role in cell cycle regulation and transcription (Sherr, 1996). The less-than impressive outcome of early clinical trials of CDK inhibitors has been attributed in part to poor pharmacology (Senderowicz et al, 1998; Nutley et al, 2005; Benson et al, 2007; Lapenna and Giordano, 2009). In the case of flavopiridol, reduced activity was due, at least in part, to low intracellular drug levels consequent to the expression of ABC transporters (Robey et al, 2001). Of general note, resistance to chemotherapy, despite initial limited response in some cases, is a substantial clinical problem accounting for treatment failure in more than 90% of patients with metastatic disease, the inevitable outcome being death (Longley and Johnston, 2005). We have recently reported novel pyrazolo[1,5-a]pyrimidine CDK inhibitors exemplified by the CDK7 selective inhibitor BS-181 (Ali et al, 2009), as well as BS-194 with preferential activity against CDK1/2/7/9 (Heathcote et al, 2010). We identified induction of the ABC transporters, ABCG2 and ABCB1, as a potential mechanism of

de novo and acquired resistance, thus reducing potency. Cells that expressed these transporters had reduced drug levels. Although it may be argued that a modest threefold induction of transporter expression in vivo (Figure 1H and I) could be overcome by dose escalation, the narrow therapeutic index of most chemotherapeutic agents may limit this option. A drug devoid of transporter activity would also be more favourable. Furthermore, analogous to the induction of acquired resistance, BS-194 induced differential receptor expression in human colon HCT-116 and human breast MCF7 cells in culture and in xenografts, with the effects in tumours occurring with a shorter latency. Although we cannot explain the mechanism for the differential receptor expression from a single drug, this phenomenon has been reported with other chemotherapeutics (Shen et al, 1986; Spoelstra et al, 1991; Cole et al, 1992; Doyle et al, 1998). Levels of expression of ABCG2 were altered with a different latency after 3 months in vitro and only after 2 weeks in vivo. Although the specific mechanism underpinning this difference is unknown, we speculate that tumour microenvironment factors may have accelerated differential

receptor expression. Hypoxia and glucose deprivation, hallmarks of tumour microenvironment, were previously shown to upregulate ABCG2 via a cis-element close to the reported HIF-1α response element at the ABCG2 promoter, co-ordinately with pre-existing MDR mechanism (Cheng and To, 2012). Consistent with previously published reports, cancer cell lines that were made resistant to conventional therapeutics such as doxorubicin and MX were also cross-resistant to BS-194 (Spoelstra et al, 1991; Ross et al, 1999). We showed that drug resistance could be reversed using pharmacological modulators of ABCG2 and ABCB1, thus demonstrating biological relevance of the transporters.

One potential mechanism of overcoming MDR phenotype may be through the inhibition of the ABC transporters; however, as each compound may have a different specificity towards one or several transporters, this strategy has significant limitations (Szakacs et al, 2006; Higgins, 2007; Fletcher et al, 2010). Several attempts have been made to develop inhibitors of the main ABC transporters, but these attempts have so far failed to provide enhanced efficacy in clinical settings (Cripe et al, 2010; Kelly et al, 2011). Another strategy may be through the rational design of compounds with the same pharmacophore that are not substrates of the ABC transporters. Using a chemical library approach, we screened a series of pyrazolo[1,5-a]pyrimidine to identify features involved in ABC transporter substrate specificity. From previous SAR studies, compounds with a MW >500 >2 aromatic rings, >8 N + O, Log$P$ between 1 and 5, a pKa >4 and PSA >85A^2 are likely to be substrates of ABCB1 and ABCG2 (Didziapetris et al, 2003; Varma et al, 2005; Kaliszczak et al, 2010). Analysis of the physicochemical properties from our series highlighted PSA (>100 Å^2) as the main factor controlling the degree of interaction with ABC transporters, which represents a higher cut-off value that has been previously described for other series (Varma et al, 2005; Kaliszczak et al, 2010). Molecular weight was below the optimal threshold for ABCB1 substrates, and the number of electron donor groups, as well as aromaticity and lipophicitity, could not discriminate the substrates from non-substrates. This suggests that very high PSA would skew the balance of determinants for ABC transporter substrate specificity. Further analysis of the SAR revealed that poor cellular permeability occurred with compounds bearing a charge at physiological pH. Although ICEC-0229 embodied most of the positive attributes discussed above and was associated with high metabolic stability, it was charged at physiological pH. Further iteration of the series led to the primary carbamate, ICEC-0782, that was uncharged at physiological pH.

Unlike ICEC-0229, ICEC-0782 was found to gain potency towards CDK2 and CDK9, while remaining active against CDK7 in the nanomolar range. This level of activity was sufficient to inhibit the phosphorylation of polII and the transcription of short-lived proteins such as Mcl-1 and cyclin D1 when tested at low micromolar concentrations. Induction of G2/M and apoptosis by ICEC-0782 were also in keeping with CDK2/7/9 inhibition. It appears that functional redundancy among CDKs and cyclin-binding partners is a frequent event bringing clear implications for the clinical utility of pan-CDK inhibition (Aleem et al, 2005; Cai et al, 2006). A growing number of studies have also reported that concomitant compromise of cell cycle and transcriptional CDK activities would have more desirable antiproliferative effects in cancer cells (Cai et al, 2006; Shapiro, 2006). The value of this strategy is exemplified by the CDK2/7/9 inhibitor SNS-032, currently in clinical development for treatment of cancer (Tong et al, 2010). The limited bioavailability of SNS-032, however, was related to its substrate specificity towards ABCB1 (Kamath et al, 2005). Analogues of SNS-032 with improved permeability have been synthesised but, to our best of our knowledge, no in vivo efficacy data are available to date (Choong et al, 2008). Phase III trials of perhaps the most advanced of the CDK inhibitors, dinaciclib (a pyrazolo[1,5-a]pyrimidine pan-CDK1/2/5/9 inhibitor

with PSA = 91 Å^2, (N + O) = 8, MW = 368 and Log$P$ = 1.38), has been initiated in patients with refractory chronic lymphocytic leukaemia comparing efficacy against ofatumumab (NCT01580228; http://clinicaltrials.gov/); however, no data on ABC transporter substrate specificity has been reported (Parry et al, 2010).

We demonstrate that ICEC-0782 is efficacious in vivo. For the HCT-116 tumour model, this efficacy profile is superior to most standard of care compounds administered as monotherapy, including 5-fluorouracil, cetuximab and oxaliplatin (Balin-Gauthier et al, 2006; Wild et al, 2006; Tumber et al, 2007). The molecular and imaging biomarkers of drug pharmacodynamics – P-Rb, phosphorylated forms of polII (P-ser2 and P-ser5) and [^{18}F]FLT–PET – validated in the present study will permit biopsy and non-invasive approach options to guide go/no-go decision in early clinical trials of ICEC-0782. Our finding that a modest 1.3-fold decrease in Ki-67 staining at 48 h was sufficient to corroborate [^{18}F]FLT–PET uptake and predict long-term outcome of ICEC-0782 (i.e., 84% tumour reduction at 14 days) was in line with previously published data (Li et al, 2012), wherein a 1.6-fold decrease in Ki-67 after 5 days of treatment with everolimus was associated with total growth inhibition at 14 days.

In aggregate, we have identified a novel pyrazolo[1,5-a] pyrimidine derivative, ICEC-0782 that recapitulated the expected biochemical behaviour of inhibiting CDK2/7/9, overcame MDR phenotype mediated by the ABC transporters and further resulted in antitumour activity. Use of imaging and molecular biochemical biomarkers of pharmacodynamics identified here will provide a rationale for the future development of ICEC-0782.

REFERENCES

Aleem E, Kiyokawa H, Kaldis P (2005) Cdc2-cyclin E complexes regulate the G1/S phase transition. Nat Cell Biol 7(8): 831–836.

Ali S, Heathcote DA, Kroll SH, Jogalekar AS, Scheiper B, Patel H, Brackow J, Siwicka A, Fuchter MJ, Periyasamy M, Tolhurst RS, Kanneganti SK, Snyder JP, Liotta DC, Aboagye EO, Barrett AG, Coombes RC (2009) The development of a selective cyclin-dependent kinase inhibitor that shows antitumor activity. Cancer Res 69(15): 6208–6215.

Balin-Gauthier D, Delord JP, Rochaix P, Mallard V, Thomas F, Hennebelle I, Bugat R, Canal P, Allal C (2006) In vivo and in vitro antitumor activity of oxaliplatin in combination with cetuximab in human colorectal tumor cell lines expressing different level of EGFR. Cancer Chemother Pharmacol 57(6): 709–718.

Benson C, White J, De Bono J, O'Donnell A, Raynaud F, Cruickshank C, McGrath H, Walton M, Workman P, Kaye S, Cassidy J, Gianella-Borradori A, Judson I, Twelves C (2007) A phase I trial of the selective oral cyclin-dependent kinase inhibitor seliciclib (CYC202; R-Roscovitine), administered twice daily for 7 days every 21 days. Br J Cancer 96(1): 29–37.

Cai D, Latham Jr VM, Zhang X, Shapiro GI (2006) Combined depletion of cell cycle and transcriptional cyclin-dependent kinase activities induces apoptosis in cancer cells. Cancer Res 66(18): 9270–9280.

Cheng GM, To KK (2012) Adverse cell culture conditions mimicking the tumor microenvironment upregulate ABCG2 to mediate multidrug resistance and a more malignant phenotype. ISRN Oncol 2012: 746025.

Choong IC, Serafimova I, Fan J, Stockett D, Chan E, Cheeti S, Lu Y, Fahr B, Pham P, Arkin MR, Walker DH, Hoch U (2008) A diaminocyclohexyl analog of SNS-032 with improved permeability and bioavailability properties. Bioorg Med Chem Lett 18(21): 5763–5765.

Cole SP, Bhardwaj G, Gerlach JH, Mackie JE, Grant CE, Almquist KC, Stewart AJ, Kurz EU, Duncan AM, Deeley RG (1992) Overexpression of a transporter gene in a multidrug-resistant human lung cancer cell line. *Science* **258**(5088): 1650–1654.

Cripe LD, Uno H, Paietta EM, Litzow MR, Ketterling RP, Bennett JM, Rowe JM, Lazarus HM, Luger S, Tallman MS (2010) Zosuquidar, a novel modulator of P-glycoprotein, does not improve the outcome of older patients with newly diagnosed acute myeloid leukemia: a randomized, placebo-controlled trial of the Eastern Cooperative Oncology Group 3999. *Blood* **116**(20): 4077–4085.

de la Motte S, Gianella-Borradori A (2004) Pharmacokinetic model of R-roscovitine and its metabolite in healthy male subjects. *Int J Clin Pharmacol Ther* **42**(4): 232–239.

Didziapetris R, Japertas P, Avdeef A, Petrauskas A (2003) Classification analysis of P-glycoprotein substrate specificity. *J Drug Target* **11**(7): 391–406.

Doyle LA, Yang W, Abruzzo LV, Krogmann T, Gao Y, Rishi AK, Ross DD (1998) A multidrug resistance transporter from human MCF-7 breast cancer cells. *Proc Natl Acad Sci USA* **95**(26): 15665–15670.

Fisher RP (2005) Secrets of a double agent: CDK7 in cell-cycle control and transcription. *J Cell Sci* **118**(Pt 22): 5171–5180.

Fletcher JI, Haber M, Henderson MJ, Norris MD (2010) ABC transporters in cancer: more than just drug efflux pumps. *Nat Rev Cancer* **10**(2): 147–156.

Harper JW, Elledge SJ (1998) The role of Cdk7 in CAK function, a retro-retrospective. *Genes Dev* **12**(3): 285–289.

Heathcote DA, Patel H, Kroll SH, Hazel P, Periyasamy M, Alikian M, Kanneganti SK, Jogalekar AS, Scheiper B, Barbazanges M, Blum A, Brackow J, Siwicka A, Pace RD, Fuchter MJ, Snyder JP, Liotta DC, Freemont PS, Aboagye EO, Coombes RC, Barrett AG, Ali S (2010) A novel pyrazolo[1,5-a]pyrimidine is a potent inhibitor of cyclin-dependent protein kinases 1, 2, and 9, which demonstrates antitumor effects in human tumor xenografts following oral administration. *J Med Chem* **53**(24): 8508–8522.

Higgins CF (2007) Multiple molecular mechanisms for multidrug resistance transporters. *Nature* **446**(7137): 749–757.

Kaliszczak M, Antonow D, Patel KI, Howard P, Jodrell DI, Thurston DE, Guichard SM (2010) Optimization of the antitumor activity of sequence-specific pyrrolobenzodiazepine derivatives based on their affinity for ABC transporters. *AAPS J* **12**(4): 617–627.

Kaliszczak M, Trousil S, Aberg O, Perumal M, Nguyen QD, Aboagye EO (2013) A novel small molecule hydroxamate preferentially inhibits HDAC6 activity and tumour growth. *Br J Cancer* **108**(2): 342–350.

Kamath AV, Chong S, Chang M, Marathe PH (2005) P-glycoprotein plays a role in the oral absorption of BMS-387032, a potent cyclin-dependent kinase 2 inhibitor, in rats. *Cancer Chemother Pharmacol* **55**(2): 110–116.

Kelly RJ, Draper D, Chen CC, Robey RW, Figg WD, Piekarz RL, Chen X, Gardner ER, Balis FM, Venkatesan AM, Steinberg SM, Fojo T, Bates SE (2011) A pharmacodynamic study of docetaxel in combination with the P-glycoprotein antagonist tariquidar (XR9576) in patients with lung, ovarian, and cervical cancer. *Clin Cancer Res* **17**(3): 569–580.

Lapenna S, Giordano A (2009) Cell cycle kinases as therapeutic targets for cancer. *Nat Rev Drug Discov* **8**(7): 547–566.

Leyton J, Alao JP, Da Costa M, Stavropoulou AV, Latigo JR, Perumal M, Pillai R, He Q, Atadja P, Lam EW, Workman P, Vigushin DM, Aboagye EO (2006) In vivo biological activity of the histone deacetylase inhibitor LAQ824 is detectable with 3′-deoxy-3′-[18F]fluorothymidine positron emission tomography. *Cancer Res* **66**(15): 7621–7629.

Li Z, Graf N, Herrmann K, Junger A, Aichler M, Feuchtinger A, Baumgart A, Walch A, Peschel C, Schwaiger M, Buck A, Keller U, Dechow T (2012) FLT-PET is superior to FDG-PET for very early response prediction in NPM-ALK-positive lymphoma treated with targeted therapy. *Cancer Res* **72**(19): 5014–5024.

Lolli G, Johnson LN (2005) CAK-cyclin-dependent activating kinase: a key kinase in cell cycle control and a target for drugs? *Cell Cycle* **4**(4): 572–577.

Longley DB, Johnston PG (2005) Molecular mechanisms of drug resistance. *J Pathol* **205**(2): 275–292.

Malumbres M, Barbacid M (2001) To cycle or not to cycle: a critical decision in cancer. *Nat Rev Cancer* **1**(3): 222–231.

Meinhart A, Kamenski T, Hoeppner S, Baumli S, Cramer P (2005) A structural perspective of CTD function. *Genes Dev* **19**(12): 1401–1415.

Nakagawa M, Schneider E, Dixon KH, Horton J, Kelley K, Morrow C, Cowan KH (1992) Reduced intracellular drug accumulation in the absence of P-glycoprotein (mdr1) overexpression in mitoxantrone-resistant human MCF-7 breast cancer cells. *Cancer Res* **52**(22): 6175–6181.

Nutley BP, Raynaud FI, Wilson SC, Fischer PM, Hayes A, Goddard PM, McClue SJ, Jarman M, Lane DP, Workman P (2005) Metabolism and pharmacokinetics of the cyclin-dependent kinase inhibitor R-roscovitine in the mouse. *Mol Cancer Ther* **4**(1): 125–139.

Palancade B, Bensaude O (2003) Investigating RNA polymerase II carboxyl-terminal domain (CTD) phosphorylation. *Eur J Biochem* **270**(19): 3859–3870.

Parry D, Guzi T, Shanahan F, Davis N, Prabhavalkar D, Wiswell D, Seghezzi W, Paruch K, Dwyer MP, Doll R, Nomeir A, Windsor W, Fischmann T, Wang Y, Oft M, Chen T, Kirschmeier P, Lees EM (2010) Dinaciclib (SCH 727965), a novel and potent cyclin-dependent kinase inhibitor. *Mol Cancer Ther* **9**(8): 2344–2353.

Pham AN, Wang J, Fang J, Gao X, Zhang Y, Blower PE, Sadee W, Huang Y (2009) Pharmacogenomics approach reveals MRP1 (ABCC1)-mediated resistance to geldanamycins. *Pharm Res* **26**(4): 936–945.

Pines J (1991) Cyclins: wheels within wheels. *Cell Growth Differ* **2**(6): 305–310.

Pisaneschi F, Nguyen QD, Shamsaei E, Glaser M, Robins E, Kaliszczak M, Smith G, Spivey AC, Aboagye EO (2010) Development of a new epidermal growth factor receptor positron emission tomography imaging agent based on the 3-cyanoquinoline core: synthesis and biological evaluation. *Bioorg Med Chem* **18**(18): 6634–6645.

Prelich G (2002) RNA polymerase II carboxy-terminal domain kinases: emerging clues to their function. *Eukaryot Cell* **1**(2): 153–162.

Robey RW, Medina-Perez WY, Nishiyama K, Lahusen T, Miyake K, Litman T, Senderowicz AM, Ross DD, Bates SE (2001) Overexpression of the ATP-binding cassette half-transporter, ABCG2 (Mxr/BCrp/ABCP1), in flavopiridol-resistant human breast cancer cells. *Clin Cancer Res* **7**(1): 145–152.

Ross DD, Yang W, Abruzzo LV, Dalton WS, Schneider E, Lage H, Dietel M, Greenberger L, Cole SP, Doyle LA (1999) Atypical multidrug resistance: breast cancer resistance protein messenger RNA expression in mitoxantrone-selected cell lines. *J Natl Cancer Inst* **91**(5): 429–433.

Senderowicz AM, Headlee D, Stinson SF, Lush RM, Kalil N, Villalba L, Hill K, Steinberg SM, Figg WD, Tompkins A, Arbuck SG, Sausville EA (1998) Phase I trial of continuous infusion flavopiridol, a novel cyclin-dependent kinase inhibitor, in patients with refractory neoplasms. *J Clin Oncol* **16**(9): 2986–2999.

Shapiro GI (2006) Cyclin-dependent kinase pathways as targets for cancer treatment. *J Clin Oncol* **24**(11): 1770–1783.

Shen DW, Fojo A, Chin JE, Roninson IB, Richert N, Pastan I, Gottesman MM (1986) Human multidrug-resistant cell lines: increased mdr1 expression can precede gene amplification. *Science* **232**(4750): 643–645.

Sherr CJ (1994) G1 phase progression: cycling on cue. *Cell* **79**(4): 551–555.

Sherr CJ (1996) Cancer cell cycles. *Science* **274**(5293): 1672–1677.

Spoelstra EC, Dekker H, Schuurhuis GJ, Broxterman HJ, Lankelma J (1991) P-glycoprotein drug efflux pump involved in the mechanisms of intrinsic drug resistance in various colon cancer cell lines. Evidence for a saturation of active daunorubicin transport. *Biochem Pharmacol* **41**(3): 349–359.

Szakacs G, Paterson JK, Ludwig JA, Booth-Genthe C, Gottesman MM (2006) Targeting multidrug resistance in cancer. *Nat Rev Drug Discov* **5**(3): 219–234.

Tong WG, Chen R, Plunkett W, Siegel D, Sinha R, Harvey RD, Badros AZ, Popplewell L, Coutre S, Fox JA, Mahadocon K, Chen T, Kegley P, Hoch U, Wierda WG (2010) Phase I and pharmacologic study of SNS-032, a potent and selective Cdk2, 7, and 9 inhibitor, in patients with advanced chronic lymphocytic leukemia and multiple myeloma. *J Clin Oncol* **28**(18): 3015–3022.

Tumber A, Collins LS, Petersen KD, Thougaard A, Christiansen SJ, Dejligbjerg M, Jensen PB, Sehested M, Ritchie JW (2007) The histone deacetylase inhibitor PXD101 synergises with 5-fluorouracil to inhibit colon cancer cell growth in vitro and in vivo. *Cancer Chemother Pharmacol* **60**(2): 275–283.

Varma MV, Sateesh K, Panchagnula R (2005) Functional role of P-glycoprotein in limiting intestinal absorption of drugs: contribution of passive permeability to P-glycoprotein mediated efflux transport. *Mol Pharm* **2**(1): 12–21.

Vichai V, Kirtikara K (2006) Sulforhodamine B colorimetric assay for cytotoxicity screening. *Nat Protoc* **1**(3): 1112–1116.

Wild R, Fager K, Flefleh C, Kan D, Inigo I, Castaneda S, Luo FR, Camuso A, McGlinchey K, Rose WC (2006) Cetuximab preclinical antitumor activity (monotherapy and combination based) is not predicted by relative total or activated epidermal growth factor receptor tumor expression levels. *Mol Cancer Ther* **5**(1): 104–113.

Workman P, Aboagye EO, Balkwill F, Balmain A, Bruder G, Chaplin DJ, Double JA, Everitt J, Farningham DA, Glennie MJ, Kelland LR, Robinson V, Stratford IJ, Tozer GM, Watson S, Wedge SR, Eccles SA (2010) Guidelines for the welfare and use of animals in cancer research. *Br J Cancer* **102**(11): 1555–1577.

Supplementary Information accompanies this paper on British Journal of Cancer website (http://www.nature.com/bjc)